Numerical Aerodynamic Analysis of a New Twin Engine Commuter Aircraft

Longitudinal and Lateral-Directional Derivatives

[Nicolosi Fabrizio, Corcione Salvatore, Della Vecchia Pierluigi, Agostino De Marco]

Abstract — **This paper deals with numerical investigation about both longitudinal and lateral-directional static aerodynamic characteristics of a new twin-engine commuter aircraft with eleven seats, Tecnam P2012. Numerical analyses have been performed on complete and many partial aircraft configurations in order to evaluate the contribution of each aircraft component and to estimate their mutual interferences. The analyses have been conducted at wind tunnel Reynolds number in order to provide a validation of the numerical investigation. Finally numerical analyses have been also performed at free flight conditions, in order to have an estimation of the Reynolds number effect in especially on the aircraft base drag coefficient and on the wing span loads in both flap up and flap down conditions.**

Keywords—CFD, Longitudinal and Lateral-Directional Stability, CommuterAaircfrat

I. Introduction

Since 2011 Tecnam Aircraft Industries (http://www.tecnam.com/Default.aspx) and researchers at DII (Department of the Industrial Engineering of the University of Naples) are deeply involved in the design of a new 11 seats commuter aircraft, the P2012 Traveller. Design guidelines, specific market opportunities, numerical aerodynamic analysis and wind-tunnel tests have been outlined by the authors in previous works [1-3]. The authors at DII have matured experience in aerodynamic design [4] and flight tests of light aircraft [5, 6] and many research activities have been performed in collaboration with Tecnam.

Nicolosi Fabrizio, Corcione Salvatore, Della Vecchia Pierluigi, Agostino De Marco

Department of Industrial Engineering/University of Naples Federico II
Italy

II. The P2012 Traveller

The Tecnam P2012 Traveller is a twin engine, 11 seats, high-wing and body mounted horizontal tail aircraft. Design specifications have led to a fixed landing gear, high cabin volume and short take-off and landing distances. The aircraft is powered by two Lycoming piston TEO-540-A1A engines. The aircraft will be used both as a passenger airplane but it has been designed to be a very versatile and flexible aerial platform, offering multi-role opportunities. More details about preliminary design phase and aerodynamic analysis have been shown by authors in previous scientific articles [1-3]. Fig. 1 shows the aircraft three views. P2012 has a straight tapered wing with surface of about 25 square meters and a wing span of about 14 meters. Two quasi symmetrical nacelles are installed on wing and two winglets are mounted at wing tip. Slender fuselage geometry of about 12 meters can accommodate up to 11 occupants (2 pilots plus 9 passengers) with an higher fineness ratio for the aircraft category equal to l_F/d_F = 7.24. P2012 main geometrical dimensions are summarized in Table I. Conventional horizontal body mounted tail plane has been adopted with a horn balanced elevator movable surface and 30 degrees sweep vertical tail plane with dorsal fin has been designed with a high control power rudder surface. The research group has performed in the past extensive activities on light and general aviation aircraft, acquiring experience in the analysis, aerodynamic design and flight testing of this particular aircraft category.

TABLE I.   P2012 MAIN GEOMETRICAL CHARACTERISTICS

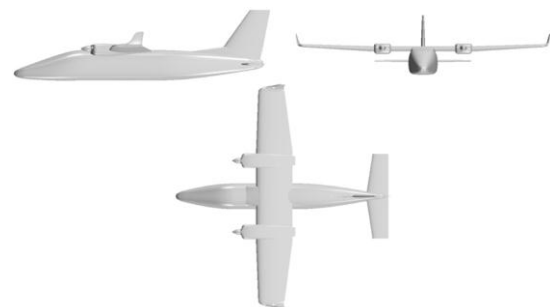| Symbol	Value
S_W	25.40 m2 (268.2 ft2)
b_W	14.00 m (45.9 ft)
AR_W	7.72
$\overline{c}$	1.87 m (6.14 ft)
λ_W	0.73
l_F	11.59 m (38.0 ft)
h_F	1.60 m (5.3 ft)
d_F	1.60 m (5.3 ft)

Figure 1.   P2012 Traveller, three views (CAD)

III. Mesh and physics setup

Aerodynamic analyses have been fulfilled through the software STAR-CCM+ [7]. The software includes all the required features from the pre-processing, to the post-processing and data analyses tools. The whole simulation procedure from the pre-processing (geometry import, mesh set-up and building, physics set-up, iteration run and post-

processing) have been completely automated through the use of macros java since the software is java language based.

A. *Geometry*

P2012 geometry has been divided into several components (such as Fuselage, Horizontal and Vertical tailplanes, Nacelles and Ogive and Wing), as shown in Fig. 2, in order to analyze different configurations.
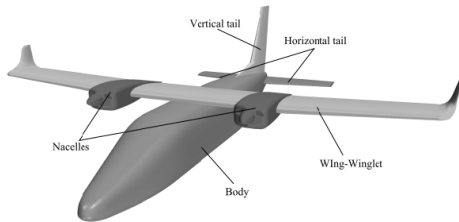

Figure 2.   P2012 Traveller numerical CAD model

The computational domain has been defined as a block with dimensions of a 10 fuselage lengths ahead the fuselage nose, 20 behind, 8 beside and 5 fuselage lengths above and below. The computational domain and boundary condition settings are shown in Fig. 3.
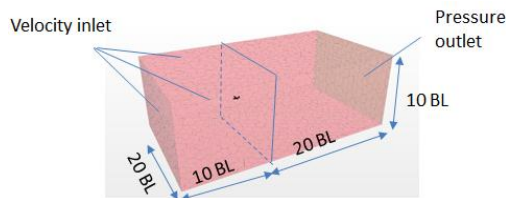

Figure 3.   Computational domain and boundary conditions setting

B. *Mesh*

The volume mesh has been built up using the "polyhedral mesher" and "prism layer option". Table II shows the main mesh parameters used to build up the mesh for the simulation. Numerical simulations have been performed both at wind tunnel tests and at free flight Reynolds number (about $0.6e^6$ and $4.5e^6$ and $9.5e^6$ respectively). The prism layer has been automated generated through macro java according with the flight conditions being simulated prescribed as input data.

TABLE II.   SURFACE REMESHER AND PRISM LAYER PARAMETERS

Surface remesher	
Parameter	**Value**
Base size (BS)	0.8m
Surface relative minimum size	0.1% BS
Surface relative target size	250%BS
Prism layer	
Parameter	**Value**
Number of prism layers	20
Near wall thickness (Re=$0.6e^6$)	$2.1e^{-5}$m
Near wall thickness (Re=$9.56e^6$)	$1.6e^{-6}$m

In order to ease the solution convergence process, some volumetric controls have been designed with the aim to improve the mesh density in that area where the surface curvatures are high (such as the lift surfaces leading edge) and along the trailing edges of the wing and tailplanes surfaces. Fig. 4 shows an example of the polyhedral mesh. The final mesh (around the complete aircraft configuration semi-model) consists of about 9millions of polyhedral cells.
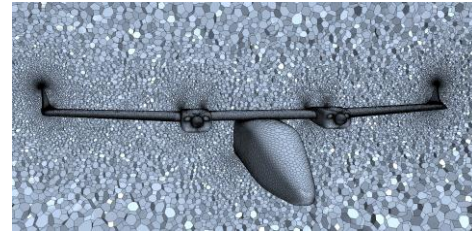

Figure 4.   Polyhedral surface and volume mesh view

C. *Physics*

Since all the simulated conditions lead the Mach number to not exceed 0.25 the flow has been considered to be incompressible (M<<1), the density has been considered to be constant and a segregated solver approach has been chosen. The Spalart-Allmaras turbulence model [8] has been used.

TABLE III.   FLUID PROPERTIES

Wind tunnel Reynolds (Re=$0.6e^6$)	
Property	**Value**
Density	1.184 kg/m^3
Dynamic viscosity	$1.855e^{-5}$ Pa-s
Free flight Reynolds (Re=$9.5e^6$)	
Property	**Value**
Density	1.184 kg/m^3
Dynamic viscosity	$1.067e^{-6}$ Pa-s

The physics set up, fluid properties, flow direction and velocity magnitude has been automated in a macro java that takes in input the flight test conditions (such as flow speed and flight altitude) and arrays of value for incidence angle and/or sideslip angle. The number of mesh cells has been changed by setting different base sizes. Tests about the numerical solution convergence with respect to the mesh number of cells have been conducted on the semi-model of the complete aircraft configuration with flap down at 40°. The goodness of the boundary layer simulation is granted by the value of the wall y^+ parameter. This parameter it is almost about 1 both at the wind tunnel and free flight Reynolds number. The total number of cells was about $9.0e^6$ for a semi-model.

IV.   **Longitudinal analysis**

Longitudinal simulations have been performed in order to evaluate aircraft stability and control characteristics and aerodynamic derivatives. Several aircraft configuration have been simulated in order to evaluate the aircraft components effect on the longitudinal stability, in particular the fuselage and nacelles contribution.

A. *Lift, pitching moment coefficient and downwash estimation*

Simulations have been performed on several configurations. In Fig. 5 the lift coefficient of several configurations is shown. As it can be seen the lift slope is slightly modified by the two nacelles, in accordance with what was shown by authors in [1, 2, 3].
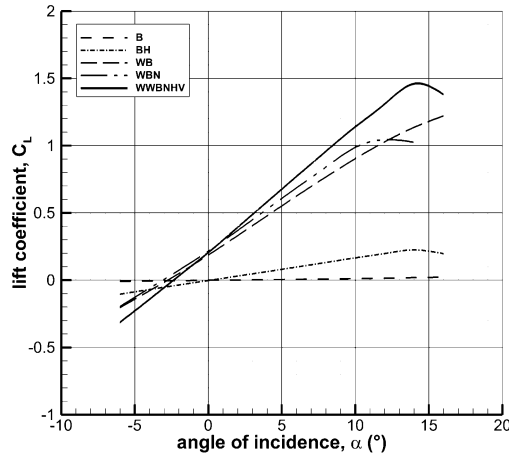
Figure 5.   Lift coefficient brakdown at Reynolds number $0.6e^6$

The measured wing-body lift slope is about $0.073\mathrm{deg}^{-1}$, while the wing-body-nacelles configuration shows a lift slope of about $0.079\mathrm{deg}^{-1}$ (see also Table IV) highlighting an almost neutral effect of the nacelle, with a behavior similar to a symmetrical airfoil also due to a higher nacelle length. As it can be seen in Fig. 6 and summarized in Table IV, the two nacelles lead to an aft shift of wing-body aerodynamic center of about 4.4% of the mean aerodynamic chord compared to the wing-body configuration.

TABLE IV.   LIFT AND PITCHING MOMENT CURVE SLOPE BREAKDOWN, RANGE OF A ϵ [0-6°]

	Numerical value
$C_{L\alpha,\ WWBNHV}$	$0.0914\mathrm{deg}^{-1}$
$C_{L\alpha,\ WB}$	$0.072\mathrm{deg}^{-1}$
$C_{L\alpha,\ WBN}$	$0.079\mathrm{deg}^{-1}$
$C_{M\alpha,\ WWBNHV}$	$-0.0249\mathrm{deg}^{-1}$
$C_{M\alpha,\ WB}$	$0.0081\mathrm{deg}^{-1}$
$C_{M\alpha,\ WBN}$	$0.0098\mathrm{deg}^{-1}$
N_0	49% $\overline{c}$
$d\varepsilon/d\alpha$	0.30
$\Delta x_{ac,B}$	12% $\overline{c}$
$\Delta x_{ac,N}$	4.4% $\overline{c}$

Complete aircraft neutral point in clean configuration is about 49% of the mean aerodynamic chord and the estimated downwash derivative is equal to 0.3. Downwash derivative has been estimated by comparing the pitching moment curve slope of the horizontal tailplane in both BH and WWBNHV configuration.
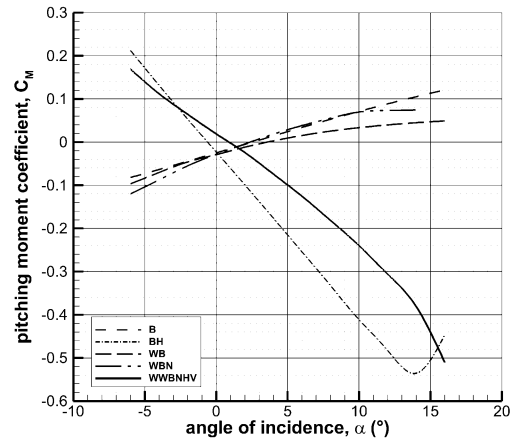
Figure 6.   Pitching moment coefficient breakdown, $Re=0.6e^6$, $x_{cg}/\overline{c} = 0.25$ $z_{cg}/\overline{c} = 0.25$ and $i_{to} = 0°$

B. *Flap effect*

Complete aircraft configuration at three flap deflections have been simulated in order to estimate the flap contribution to lift and especially to longitudinal stability characteristics. Tested flap deflections with flap up (retracted) configuration, flap deflection of 15° and full flap deflection of 40° are representative of cruise, take-off and landing condition respectively. Fig. 7 shows the lift coefficient variation with respect to the aircraft angle of attack highlighting the increase of the lift coefficient at zero angle of attack. The flap deflection leads to an increase of the lift curve slope of about 10%, as it is also outlined in Table V. Flap deflections lead to a lift coefficient increment of about 0.3 and 0.8 at zero angle of attack in takeoff and landing condition respectively. The maximum lift coefficient is increased of about 0.15 and 0.7 in take-off and landing conditions respectively Fig. 8 shows instead the pitching moment coefficient with respect to the lift coefficient. Areas of a sensible reduction in the longitudinal stability can be found in the full flap condition and low angles of attack, where the interaction of the wing wake with the horizontal tailplane became stronger leading to both a reduction in the local dynamic pressure and an increased value of the downwash angle of the flow coming from the wing. Table V also illustrates the neutral point location in terms of mean aerodynamic chord at typical lift coefficients and outlines the effect of flap both in the zero angle of attack lift coefficient and in the zero lift drag coefficient (last column of Table V).

TABLE V.   FLAP EFFECT ON COMPLETE AIRCRAFT CONFIGURATION, RE=0.6E6.

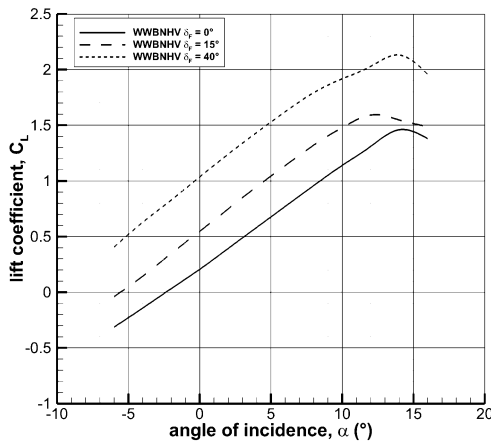|	$C_{L\alpha}\ \mathrm{deg}^{-1}$ (α ϵ [0°-6°])	N_0 (% $\overline{c}$)	ΔC_{L0}
WWBNHV $\delta_F = 0°$	0.0914	49(@C_L=0.4)	---
WWBNHV $\delta_F = 15°$	0.1000	54.7(@C_L=1.0)	0.32
WWBNHV $\delta_F = 40°$	0.1010	50.1(@C_L=1.6)	0.83

Figure 7.   Complete aircraft at three flap delfection, lift coefficient versus angle of incidence
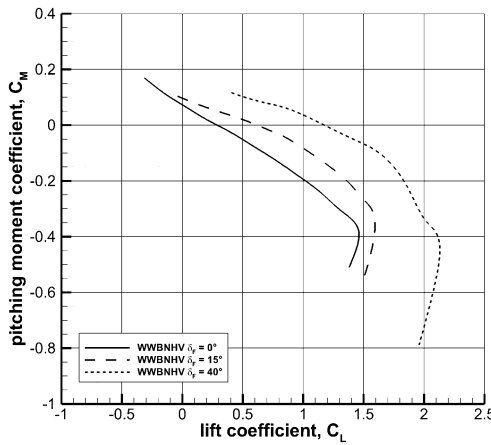

Figure 8.   Complete aircraft at three flap delfection, pitching moment coefficient versus lift coefficient

C.   *Free Flight Reynolds and Wing loads*

Cruise and stall Reynolds number have been tested and results compared. As it is clearly outlined in Fig. 9, the maximum lift coefficient increases of about 13% at Reynolds number of $9.5e^6$. Simulations performed at the free flight Reynolds number has also led to a more reliable estimation of the drag breakdown and basic drag coefficient of the aircraft. Fig. 10 shows the comparison between the contributions to the C_{D0} of each aircraft component estimated at both wind tunnel and cruise Reynolds number ($0.6e^6$ Fig. 10a, $9.5e^6$ Fig. 10b). A basic drag coefficient of about 240 drag counts can be estimated at the cruise Reynolds number. Fig. 10 also shows the aircraft components contribution to C_{D0} broken down into both contributes of shear and pressure. Simulation performed at free flight Reynolds number have also led to the estimation of the wing loads, a very useful data to the preliminary design and sizing of the wing structure. This has been clearly highlighted by numerical analyses. As matter of fact wing span loads have been extracted from the simulation for several aircraft configurations. Many effects concerning the aerodynamic behavior of wing-fuselage junction and winglet have confirmed previous analysis performed on regional turboprop configurations [9]. Some analysis on the correction of zero-lift drag coefficient has been performed following indications from [10]. Investigation of winglet effect on Oswald factor has been performed and brought to similar results as other previous investigations on wing-tip effects [11].
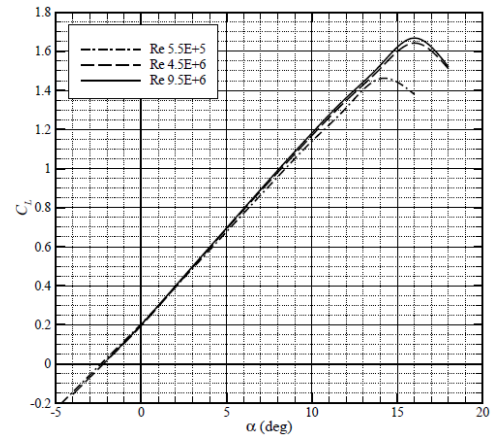

Figure 9.   Reynolds number effect on lift coefficient

The simulation at free-flight Reynolds number shows that the stall to happen at 18° incidence and the first section affected by the occurrence of the stall is placed immediately before the nacelle, as illustrated by the streamlines of Fig. 11 and clearly highlighted by the wing load distribution illustrated in Fig. 12.
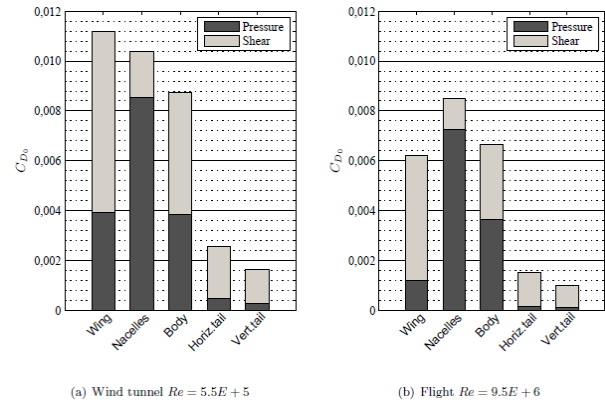

(a) Wind tunnel $Re = 5.5E + 5$ (b) Flight $Re = 9.5E + 6$

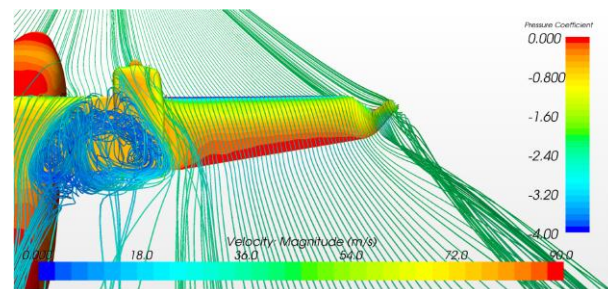Figure 10. Bar chart of C_{D0} of each aircfat component, shear and pressure breakdown

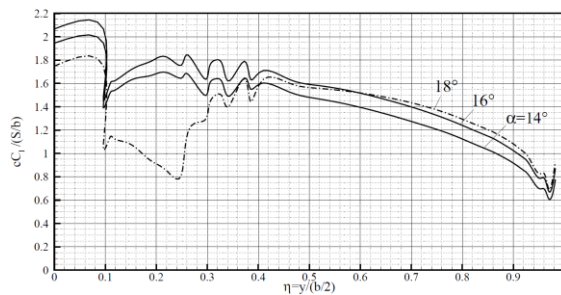Figure 11. Stremlines on the wing at Re=9.5e^6 at 18° of incidence

Figure 12. Wing span loads at Re=0.6e^6 at different angle of incidence

V.   Lateral-directional analysis

Simulation of the complete aircraft at several rudder deflections, have been performed in order to estimate both lateral-directional and control derivatives.
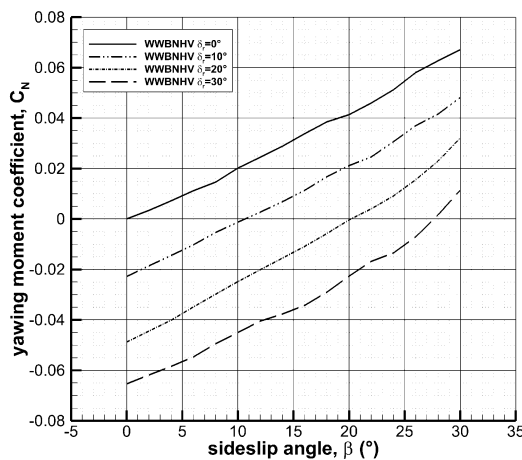

Figure 13. Complete aircraft yawing moment coefficient at several rudder deflections, Re=0.6e^6

Fig. 13 shows the yawing moment variation with respect to the sideslip angle at several rudder deflections. The complete aircraft shows a directional stability of about 0.00183deg^{-1}, while the control derivative is about 0.00230deg^{-1} in the linear range of rudder effectiveness. The results of lateral-directional CFD analysis concerning the directional stability and vertical tail behavior, have also confirmed the interference effects previously highlighted in previous articles[12-14]. Fig. 14 shows instead the variation of the complete aircraft rolling moment coefficient with respect to the sideslip angle. The lateral stability derivatives of the complete aircraft is about 0.00250deg^{-1} with winglet on configuration while in the winglet off configuration is about 0.00154deg^{-1}, this means that the winglet increase the lateral stability of about 60%, this is quite higher than both what authors have experimentally measured in [3] and what can be estimated by applying the approach suggested in [15].

VI.   Conclusion

The automated procedure with java macros allows evaluating in a relative rapid manner the aerodynamic characteristics of a complete aircraft in several configurations

and attitudes. Very useful information can be automatically extracted in the CFD software, such as wing loads, stall pattern and stability and control characteristics.
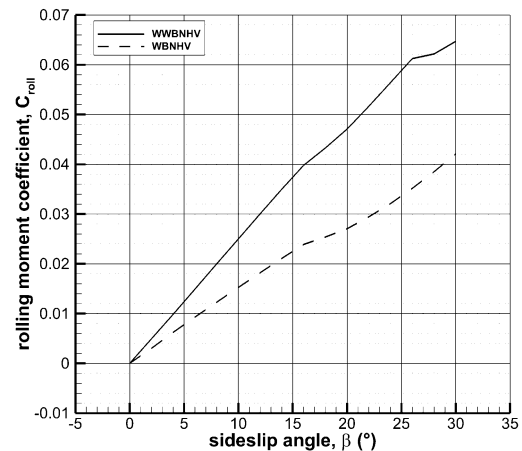

Figure 14. Winglet effect on lateral stability, Re=0.6e^6

References

[1] Nicolosi F., Della Vecchia P. and Corcione S., "Design and Aerodynamic Analysis of a Twin-engine Commuter Aircraft", Aerospace Science and Technology (Elsevier), Vol. 40, Jan. 2015, pp.1-16, doi: 10.1016/j.ast.2014.10.008.

[2] Nicolosi F., Della Vecchia P. and Corcione S., "Aerodynamic analysis and Design of a twin engine commuter aircraft", proceedings of 28th ICAS Conference, 2012, Brisbane, Australia, ISBN: 9780956533319.

[3] Nicolosi F., Corcione S. and Della Vecchia P., "Commuter Aircraft Aerodynamic Design: Wind-Tunnel tests and CFD Analysis", proceedings of the 29th ICAS Conference, St. Petersburg (Russia), 2014, pp. 1-13, Proc. ISBN 3-932182-80-4.

[4] Coiro, D.P., Nicolosi, F. Grasso, F. "Design and Testing of Multi-Element Airfoil for Short-Takeoff-and-Landing Ultralight Aircraft, " *Journal of Aircraft*, Vol. 46, N. 5, Sept.-Oct. 2009, pp. 1795-1807. ISSN 0021-8669. doi: 10.2514/1.43429.

[5] Nicolosi, F., De Marco, A., Della Vecchia, P. "Flight Tests, Performances and Flight Certifcation of a Twin-Engine Light Aircraft, " *Journal of Aircraft*, Vol. 48, N. 1, January-February 2011, pp. 177-192. ISSN 0021-8669. doi: 10.2514/1.C031056

[6] Nicolosi, F., De Marco, A., Della Vecchia, P. "Stability, Flying Qualities and Longitudinal Parameter Estimation of a Twin-Engine CS23 Certified Light Aircraft, " *Aerospace Science and Technology (Elsevier)* AESCTE 2734, Vol. 24, N. 1, January–February 2013, pp. 226-240. ISSN 1270-9638. doi: 10.1016/j.ast.2011.11.011

[7] CD-adapco. STAR-CCM+ User Guide. CD-adapco, 2013.

[8] P.R. Spalart, S.R. Allmaras, A One-equation Turbulence Model for Aerodynamic Flows, 1992, American Institute of Aeronautics and Astronautics.

[9] Della Vecchia, P., Nicolosi, F. "Aerodynamic guidelines in the design and optimization of new regional turboprop aircraft, " *Aerospace Science and Technology (Elsevier)* AESCTE Vol. 38 , October 2014, pp. 88-104, ISSN 1270-9638. doi: 10.1016/j.ast.2014.07.018.

[10] J. Roskam, Airplane flight dynamics and automatic flight controls, part 1, Design Analysis and Research Corporation, 2003.

[11] Coiro, D.P., Nicolosi, F., Scherillo, F., Maisto, U. "Improving Hang-Glider Maneuverability using multiple winglets: a numerical and experimental investigation, " *Journal of Aircraft*, Vol. 45, N. 3, May-June 2008, pp. 981-989. ISSN 0021-8669. doi: 10.2514/1.33265

[12] Nicolosi, F., Della Vecchia, P., Ciliberti, D. "An investigation on vertical tailplane contribution to aircraft sideforce. " *Aerospace Science and Technology (Elsevier)* AESCTE 2873, Vol. 28, N. 1, July 2013, pp. 401–416, ISSN 1270-9638. doi: 10.1016/j.ast.2012.12.006

[13] Nicolosi, F., Della Vecchia, P., Ciliberti, D. "Aerodynamic interference issues in aircraft directional control, " *ASCE's Journal of Aerospace Engineering*, Vol. 28, N. 1, Jan. 2015, ISSN 0893-1321. doi: 10.1061/(ASCE)AS.1943-5525.0000379 , 04014048

[14] Nicolosi, F., Della Vecchia P., Ciliberti D., Cusati V."*Development of new Preliminary Design Methodologies for Regional Turboprop Aircraft by CFD Analysis*", 29th ICAS Conference, St. Petersburg (Russia), 07-12 September 2014, pp. 1-11. ISBN 3-932182-80-4

[15] Nickel K. and Wohlfahrt M., "Tailless Aircraft in Theory and Practice" 1994, ,American Institute of Aeronautics and Astronautics, Washington D.C., ISBN: 1563470942.